

# The Mechanics Analysis of Desquamation for Thermal Protection System (TPS) Tiles of Spacecraft

Zhang Taihua<sup>1,2</sup>, Meng Xianhong<sup>2</sup> and Zhang Xing<sup>2</sup>

<sup>1</sup>Academy of Opto-Electronics, Chinese Academy of Sciences, Beijing 100080

<sup>2</sup>The Institute of Solid Mechanics, Beihang University, Beijing 100083  
China

## 1. Introduction

On the basis of solid mechanics, the “Peeling off” problem of TPS tiles on space craft surface is investigated. After considering the existence of peeling stress along the interface between the TPS tiles and the frame of space shuttle, a new model of mechanics is established to satisfy the boundary conditions of shear stress, which cannot be satisfied by the traditional shear-lag model. According to these new solutions, the reasonable explanation can be made about the failure of glued joint for TPS tiles. The stress distributions are studied when TPS tiles working in high temperature condition have different length, thickness, and material, and some advices can be provided to the design of TPS tiles.

## 2. Background

Various spacecrafts have their own characteristics. For example, as for as the Thermal Protection System (TPS) is concerned, their protection programs and materials are not identical. As the main material of spacecraft structure is aluminium, the temperature of the crucial structure could not be higher than 177°C to ensure that the connection between the spacecraft internal structure and the TPS tiles with sufficient strength.

Ceramic TPS tiles plays a great role of protecting the internal structure while spacecraft is re-entering the atmosphere. But in recent years, there have been many accidents and potential dangers, even tragic plane crash tragedy without any survivals during the spacecraft re-entry. For example, in 2003 the Space Shuttle *Columbia* Accident Investigation Board determined that a hole was punctured in the leading edge on one of *Columbia*'s wings, made of TPS tiles with carbon-carbon composite. The hole had formed when a piece of insulating foam from the external fuel tank peeled off during the launch 16 days earlier and struck the shuttle's wing. During the intense heat of re-entry, hot gases penetrated the interior of the wing, destroying the support structure and causing the rest of the shuttle to break apart (XING, 2003).

Of course, the desquamation of the TPS may be induced by many reasons, such as spacecraft vibration, engine noise, external rain, hail impact and so on. In the paper, the characteristics of the working TPS tiles are studied, the effects on the peeling stress by the

feature of TPS tile's working leading stress and the different levels of aerodynamic heating are analyzed too. And then, the influence of the TPS tile's size, thickness and material designing on the peeling stress are further analyzed. Then an explanation for TPS tiles desquamation is made, and some available mechanical reference frame and recommendations during the TPS tiles designing process are attempted to provide. A sketch of glue joint with TPS tiles is shown as Figure 1.

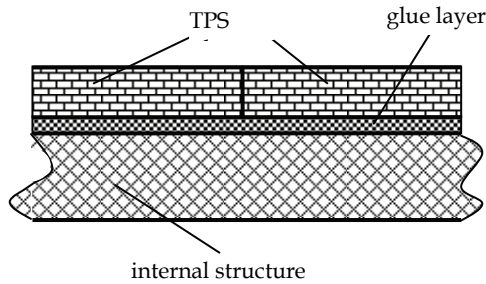


Fig. 1. A sketch of glue joint with TPS tiles

### 3. The mechanics analysis of desquamation for TPS tiles

#### 3.1 The method of analysis

Based on the analysis above, it can be seen from mechanical perspective that the problem of the desquamation for TPS tiles can be solved by analyzing the stress situation of tiles, glue layer and internal structure, as well as the relation between the internal stress and the exterior aerodynamic heating or the tiles size designing and so on. Because the TPS tiles and the internal structure are connected by the glue layer, the peeling stress, one potential factor of the peeling off of the tiles, can be obtained by analyzing the stress situation of glue layer. For this connection, to analyze glue layer stresses and confirm the strength of the joint, one can usually adopt the traditional Shear - lag Theory (Kuhn P., 1956), in which the glue layer can only suffer the shearing force while tiles and the internal structure body are only imposed on pulling force, obtaining the maximum of the glue layer shearing at its two ends. However, it is clear that this kind of analysis results can not satisfy the boundary conditions at both ends of the glue layer according to the the shear stresses reciprocal theorem, which states that the shear stresses at the ends must vanish. This article tries to provide some

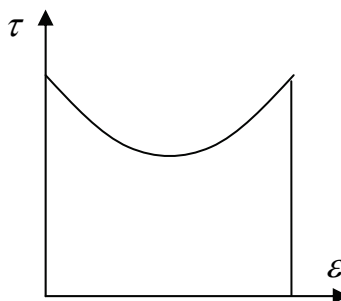


Fig. 2. Shear stress distribution along the semi-glue layer of right hand side

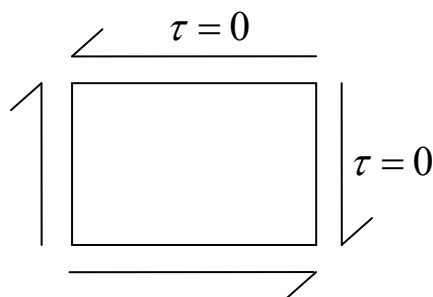


Fig. 3. Boundary condition at glue layer terminal of right hand side

reliable and advantageous mechanics basics for TPS tiles designing by studying the effects of the outside aerodynamic heating and the tiles size design on the glue layer stress but under the satisfactory of these boundary conditions.

Further, structure model shown in Figure 1 can be simplified to that shown in Figure 4(a), because the glue layer thickness is much smaller than that of tiles and structure. For the clarity, TPS tiles are marked by 1 and the internal structure by 2. In order to ensure that the layer shown Figure 4(a) could meet the boundary conditions of stress distribution, we established the following mechanical model (ZANG., 2006):

1. As shown in Figure 4(b), on the TPS tiles and the internal structure cross-sections, there is not only tension, but also bending moment and shear.
2. The glue layer thickness is ignored; however, it is assumed that the normal stress and shear stress both exists in the glue layer, as shown Figure 4(c);
3. In the connection of the TPS tiles and the structure, the longitudinal normal stress due to the tensile force and bending moment is calculated by the engineering beam theory, while the shear stress due to the elasticity of shear by the generic elasticity theory.

On this basis, we can solve the problem by force method :

1. Regard the tile's pulling stress and bending moment as generalized internal force, which is utilized to express the other internal force and stress by the equilibrium equations including tensile structure and the bending moment and glue layer's shear stresses and direct stress.
2. Establish the compatible equations which should be satisfied by the above two generalized internal force, two second order differential Eulerian equations satisfied by pulling force and bending moment, according to the complementary virtual work principle.
3. Obtain the closed analytical solution of generalized internal force and the glue layer stress by solving these two Eulerian equations under the boundary conditions.

### 3.2 Equilibrium equations

First, consider a cross-section having a distance  $x$  from the symmetry plane of the TPS tile, as shown in Figure 4(a), and regard the right part as one free body as shown in Figure 4(b). Obviously, the axial force  $N_1$  and bending moment  $M_1$  of the TPS tiles can be considered as the redundant internal forces of constrains for the equilibrium equations, which are both the function of  $x$ .

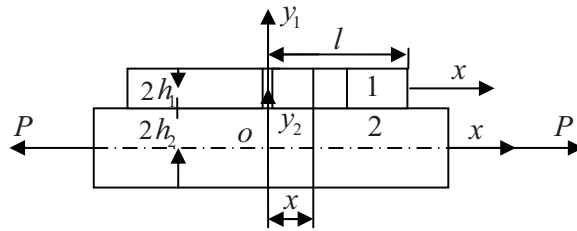


Fig. 4. (a) Coordinate systems of glue joint with mono-lateral connecting plate

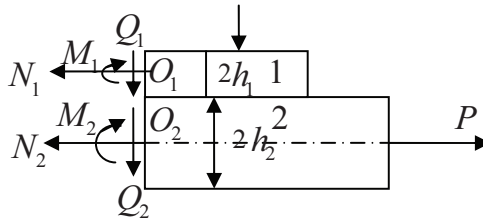


Fig. 4(b) Force state at cross section  $x$  of glue joint

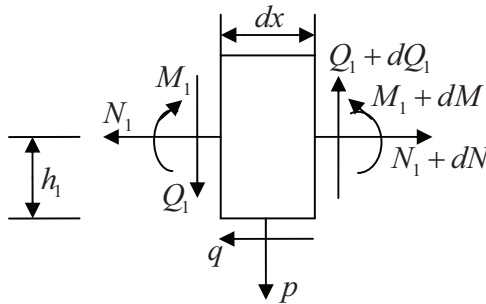


Fig. 4. (c) Free body diagram of infinitesimal segment  $dx$  along the connecting plate

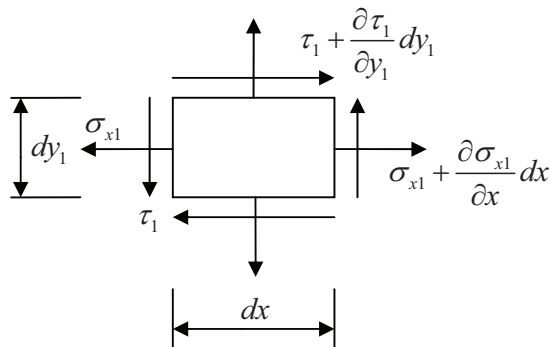


Fig. 4. (d) Free body diagram of infinitesimal element  $dx \times dy_1$  within the connecting plate

$$N_1 = N(x) = N \tag{1}$$

$$M_1 = M(x) = M \tag{2}$$

It can be seen by applying equilibrium equations to the free body that the axial force  $N_2$  and bending moment  $M_2$  are respectively equal to

$$N_2 = P - N \tag{3}$$

$$M_2 = N(h_1 + h_2) - M \tag{4}$$

Then the shear layer flow  $q$  in TPS tile 1 can be obtained by applying the equilibrium equations to the free body, as shown in Figure 4(c).

$$q = \frac{dN}{dx} \tag{5}$$

It should be noted that  $q$  shall be recessed shear stress for the plate that has a unit width. Further, taking into account formula (5), the shear  $Q_1$  in the TPS tiles equals to

$$Q_1 = qh_1 - \frac{dM}{dx} = h_1 \frac{dN}{dx} - \frac{dM}{dx} \tag{6}$$

According to equilibrium equations for the free body shown in Figure 4(b) and formula (6), the shear  $Q_2$  in the structure is

$$Q_2 = -Q_1 = \frac{dM}{dx} - h_1 \frac{dN}{dx} \tag{7}$$

The normal stress  $p$  in the TPS tile layer can be obtain by the equilibrium equation for the free body, as shown in Figure 4(c).

$$p = \frac{dQ_1}{dx} = h_1 \frac{d^2N}{dx^2} - \frac{d^2M}{dx^2} \tag{8}$$

The normal stress  $\sigma_{x1}$  and shear stress  $\tau_1$  of the plate 1 should satisfy the following equation by the equilibrium conditions of an infinitesimal element that has a  $dx$  width and  $dy$  length.

$$\frac{\partial \sigma_{x1}}{\partial x} + \frac{\partial \tau_1}{\partial y_1} = 0 \tag{9}$$

According to the theory of beam (HU, 1980), we have

$$\sigma_{x1} = \frac{N_1}{A_1} - \frac{M_1}{I_1} y_1 = \frac{N}{A_1} - \frac{M}{I_1} y_1 \tag{10}$$

Inserting equation (10) into equation (9) and taking into account the following boundary conditions results in

$$y_1 = h_1, \quad \tau_1 = 0 \quad (11)$$

The integration is available

$$\tau_1 = \frac{1}{A_1} \frac{dN}{dx} (h_1 - y_1) - \frac{1}{2I_1} \frac{dM}{dx} (h_1^2 - y_1^2) \quad (12)$$

where  $A_1$  and  $I_1$  are the cross-sectional area and axial inertia moment of the TPS tile 1 respectively.

Similarly, for the structure 2, we have

$$\frac{\partial \sigma_{x2}}{\partial x} + \frac{\partial \tau_2}{\partial y_2} = 0 \quad (13)$$

$$\sigma_{x2} = \frac{N_2}{A_2} - \frac{M_2}{I_2} y_2 = \frac{1}{A_2} (P - N) - \frac{1}{I_2} \{N(h_1 + h_2) - M\} y_2 \quad (14)$$

$$y_2 = -h_2, \quad \tau_2 = 0 \quad (15)$$

$$\tau_2 = \frac{1}{A_2} \frac{dN}{dx} (h_2 + y_2) - \frac{1}{I_2} \left\{ \frac{dN}{dx} (h_1 + h_2) - \frac{dM}{dx} \right\} \frac{1}{2} (h_2^2 - y_2^2) \quad (16)$$

In summary, according to the balance equation and the beam theory, the stress in glued pieces can be written in the following form:

$$\sigma_{x1} = \eta_{1n} N + \eta_{1m} M + \eta_{1p} P \quad (17)$$

$$\tau_1 = \zeta_{1n} \frac{dN}{dx} + \zeta_{1m} \frac{dM}{dx} \quad (18)$$

$$\sigma_{x2} = \eta_{2n} N + \eta_{2m} M + \eta_{2p} P \quad (19)$$

$$\tau_2 = \zeta_{2n} \frac{dN}{dx} + \zeta_{2m} \frac{dM}{dx} \quad (20)$$

$$q = \frac{dN}{dx} \quad (21)$$

$$p = h_1 \frac{d^2 N}{dx^2} - \frac{d^2 M}{dx^2} \quad (22)$$

In the equations above

$$\eta_{1n} = \frac{1}{A_1}, \quad \eta_{1m} = -\frac{y_1}{I_1}, \quad \eta_{1p} = 0 \quad (23)$$

$$\zeta_{1n} = \frac{1}{A_1} (h_1 - y_1), \quad \zeta_{1m} = -\frac{1}{2I_1} (h_1^2 - y_1^2) \quad (24)$$

$$\left. \begin{aligned} \eta_{2n} &= -\frac{1}{A_2} - \frac{1}{I_2}(h_1 + h_2)y_2 \\ \eta_{2m} &= \frac{y_2}{I_2}, \quad \eta_{2p} = \frac{1}{A_2} \end{aligned} \right\} \quad (25)$$

$$\left. \begin{aligned} \zeta_{2n} &= \frac{1}{A_2}(h_2 + y_2) - \frac{1}{2I_2}(h_1 + h_2)(h_2^2 - y_2^2) \\ \zeta_{2m} &= \frac{1}{2I_1}(h_2^2 - y_2^2) \end{aligned} \right\} \quad (26)$$

**3.3 Aerodynamic heating load equivalent strain**

When space craft return to the atmosphere at a high speed , it will happen that a fierce friction with the dense atmosphere produces a lot of pneumatic hot. To ensure the normal work of the interior structure of spacecraft, the tiles internal structure temperature must below 177 °C. Thus, the external tiles suffers a high-temperature heat and deforms, while the internal architecture suffers a low temperature heat and then deforms, and the deviation of the internal and external displacement caused by aerodynamic heating leads to a potential impetus to the desquamation of the tiles.

Here, we analyze the additional load generated by aerodynamic heating.

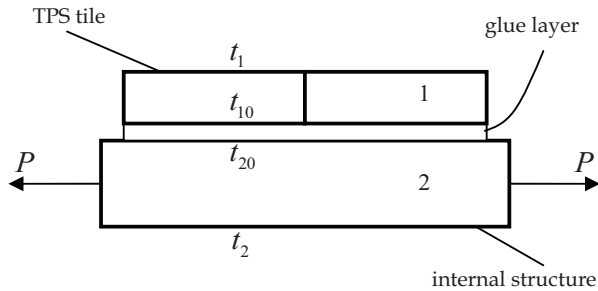


Fig. 5. The sketch of temperature between TPS tiles and structure

Let  $t_0$  denote the initial temperature while the spacecraft begins working,  $t_{j0}$  the temperature of the connection of the plate  $j$  at working state and the layer. Specifically, as shown in Figure 5,  $t_1$  is the local aerodynamic heating temperature of the outer surface of the TPS tiles and  $t_2$  is the internal temperature of the structure. For a homogeneous material, the temperature can be assumed to change approximately linearly in the thickness direction. Therefore, the local temperature can be expressed by:

$$t_j = t_{j0} + \frac{dt_j}{dy_j} y_j \quad (27)$$

Furthermore, the strain caused by the temperature should be

$$\varepsilon_{t_j} = \alpha_j (t_j - t_0) \quad (28)$$

Where,  $\alpha_j$  is the thermal expansion coefficient of board  $j$ . Inserting equation (27) into equation (28) results in

$$\varepsilon_{t_j} = \alpha_j(t_{j0} - t_0) + \alpha_j \frac{dt_j}{dy_j} y_j \quad (29)$$

Due to the linear change of the internal material temperature,

$$k_j = \alpha_j \frac{dt_j}{dy_j}, \quad \varphi_j = \alpha_j(t_{j0} - t_0) \quad (30)$$

$k_j$ , the temperature gradient of the structure  $j$ , should be a constant. Then equation (29) can be written as:

$$\varepsilon_{t_j} = \varphi_j + k_j y_j \quad (31)$$

Which the additional strain of board  $j$  is caused by aerodynamic heating.

Since the main material of the internal structure is aluminium, which has a high thermal conductivity, the temperature of the internal layer can be assumed to be the same everywhere, i.e. the temperature gradient is 0, that is

$$t_2 = t_{20}, \quad k_2 = 0 \quad (32)$$

As the layer of tiles is much thinner than the protective layer and internal structure, the temperature at the joint of the protective layer and the TPS tiles can be thought to be the same as that at the joint of the protective layer and the internal structure. Thus

$$t_{10} = t_{20} \quad (33)$$

### 3.4 Compatibility equation

The stress of TPS tiles, structure and the glue layer are all determined by the axial force and bending moment. Thus, to build expression between the former and the latter, the compatibility equations is needed, which is derived according to complementary virtual work principle due to the complexity of the deformation (Timoshenko S., 1958; HU, 1980; ZHANG, 1995; QIAN, 1980).

It can be found from (17) and (22) that the stress of the protection tiles, the structure and the layer is all depend on  $N$  and  $M$ . The compatibility equation must be introduced here in order to determine these two functions. We established the compatibility equation based on the complementary virtual work principle to deal with the complexity of deformation. Let  $\varepsilon_j$  and  $\gamma_j$  denote respectively the normal and shear strain of board  $j$ . Then the complementary virtual work principle can be expressed as

$$\delta W_c = \sum_{j=1}^2 \int_0^l \int_{-h_j}^{h_j} \{ \varepsilon_j \delta \sigma_j + \gamma_j \delta \tau_j \} dy_j dx = 0 \quad (34)$$

Where  $\delta W_c$  represents the virtual work variation of  $W_c$ ;  $\delta \sigma_j$  and  $\delta \tau_j$  representing the stress and shear stress variation of board  $j$ .



It can be seen from (17) and (20) that

$$\left. \begin{aligned} \delta\sigma_1 &= \delta\sigma_{x1} = \eta_{1n}\delta N + \eta_{1m}\delta M \\ \delta\tau_1 &= \zeta_{1n}\frac{d\delta N}{dx} + \zeta_{1m}\frac{d\delta M}{dx} \end{aligned} \right\} \quad (35)$$

$$\left. \begin{aligned} \delta\sigma_2 &= \delta\sigma_{x2} = \eta_{2n}\delta N + \eta_{2m}\delta M \\ \delta\tau_2 &= \zeta_{2n}\frac{d\delta N}{dx} + \zeta_{2m}\frac{d\delta M}{dx} \end{aligned} \right\} \quad (36)$$

Equation (34), taking into account equations (35) and (36), can be written as:

$$\begin{aligned} \delta W_c &= \sum_{j=1}^2 \int_0^l \left\{ \int_{-h_j}^{h_j} \varepsilon_j \eta_{jn} dy_j \right\} \delta N dx + \sum_{j=1}^2 \int_0^l \left\{ \int_{-h_j}^{h_j} \varepsilon_j \eta_{jm} dy_j \right\} \delta M dx \\ &+ \sum_{j=1}^2 \int_0^l \left\{ \int_{-h_j}^{h_j} \gamma_j \zeta_{jn} dy_j \right\} \frac{d\delta N}{dx} dx + \sum_{j=1}^2 \int_0^l \left\{ \int_{-h_j}^{h_j} \gamma_j \zeta_{jm} dy_j \right\} \frac{d\delta M}{dx} dx = 0 \end{aligned} \quad (37)$$

Integrating the third and fourth term by parts and taking into account

$$x = 0, \quad \delta N = 0, \quad \delta M = 0 \quad (38)$$

$$x = l, \quad \delta N = 0, \quad \delta M = 0 \quad (39)$$

And the arbitrariness and independence of  $\delta N$  and  $\delta M$  in interval  $0 < x < l$ , one can obtain the following compatibility equation, which is expressed by the strain:

$$\frac{d}{dx} \left\{ \sum_{j=1}^2 \int_{-h_j}^{h_j} \gamma_j \zeta_{jn} dy_j \right\} - \sum_{j=1}^2 \int_{-h_j}^{h_j} \varepsilon_j \eta_{jn} dy_j = 0 \quad (40)$$

$$\frac{d}{dx} \left\{ \sum_{j=1}^2 \int_{-h_j}^{h_j} \gamma_j \zeta_{jm} dy_j \right\} - \sum_{j=1}^2 \int_{-h_j}^{h_j} \varepsilon_j \eta_{jm} dy_j = 0 \quad (41)$$

where  $\varepsilon_{t_j}$  is the additional strain by aerodynamic heating.

In the case of aerodynamic heating, when the TPS tiles and structure work in the elastic range, from (17) to (20) with (31), we have

$$\varepsilon_j = \frac{1}{E_j} (\eta_{jn} N + \eta_{jm} M + \eta_{jp} P) + \varepsilon_{t_j} \quad (42)$$

$$\gamma_j = \frac{\tau_j}{G_j} = \frac{1}{G_j} (\zeta_{jn} \frac{dN}{dx} + \zeta_{jm} \frac{dM}{dx}) \quad (43)$$

Inserting (42) and (43) into (40) and (41) will result in the two compatibility equations, which are expressed by the axial force  $N$  and bending moment of the protective layer:

$$\alpha_{nm} \frac{d^2 N}{dx^2} + \alpha_{nm} \frac{d^2 M}{dx^2} - \beta_{nn} N - \beta_{nm} M = \beta_{np} P + \beta_{nt} = \beta_{np} \left( P + \frac{\beta_{nt}}{\beta_{np}} \right) \quad (44)$$

$$\alpha_{mm} \frac{d^2 N}{dx^2} + \alpha_{mm} \frac{d^2 M}{dx^2} - \beta_{mn} N - \beta_{mm} M = \beta_{mp} P + \beta_{mt} = \beta_{mp} \left( P + \frac{\beta_{mt}}{\beta_{mp}} \right) \quad (45)$$

In equation (44) and type (45),  $\beta_{nt} / \beta_{np}$  and  $\beta_{mt} / \beta_{mp}$  can be considered as additional loads caused by aerodynamic heating.

$$\left. \begin{aligned} \alpha_{nn} &= \sum_{j=1}^2 \frac{1}{G_j} \left\{ \int_{-h_j}^{h_j} \zeta_{jn} \zeta_{jn} dy_j \right\} \\ \alpha_{nm} &= \sum_{j=1}^2 \frac{1}{G_j} \left\{ \int_{-h_j}^{h_j} \zeta_{jn} \zeta_{jm} dy_j \right\} \\ \beta_{nn} &= \sum_{j=1}^2 \frac{1}{E_j} \left\{ \int_{-h_j}^{h_j} \eta_{jn} \eta_{jn} dy_j \right\} \\ \beta_{nm} &= \sum_{j=1}^2 \frac{1}{E_j} \left\{ \int_{-h_j}^{h_j} \eta_{jn} \eta_{jm} dy_j \right\} \\ \beta_{np} &= \sum_{j=1}^2 \frac{1}{E_j} \left\{ \int_{-h_j}^{h_j} \eta_{jn} \eta_{jp} dy_j \right\} \\ \beta_{nt} &= \sum_{j=1}^2 \int_{-h_j}^{h_j} (\varphi_j + k_j y_j) \eta_{jn} dy_j \end{aligned} \right\} \quad (46)$$

$$\left. \begin{aligned} \alpha_{mm} &= \sum_{j=1}^2 \frac{1}{G_j} \left\{ \int_{-h_j}^{h_j} \zeta_{jm} \zeta_{jm} dy_j \right\} \\ \alpha_{mn} &= \sum_{j=1}^2 \frac{1}{G_j} \left\{ \int_{-h_j}^{h_j} \zeta_{jm} \zeta_{jn} dy_j \right\} \\ \beta_{mn} &= \sum_{j=1}^2 \frac{1}{E_j} \left\{ \int_{-h_j}^{h_j} \eta_{jm} \eta_{jn} dy_j \right\} \\ \beta_{mm} &= \sum_{j=1}^2 \frac{1}{E_j} \left\{ \int_{-h_j}^{h_j} \eta_{jm} \eta_{jm} dy_j \right\} \\ \beta_{mp} &= \sum_{j=1}^2 \frac{1}{E_j} \left\{ \int_{-h_j}^{h_j} \eta_{jm} \eta_{jp} dy_j \right\} \\ \beta_{mt} &= \sum_{j=1}^2 \int_{-h_j}^{h_j} (\varphi_j + k_j y_j) \eta_{jm} dy_j \end{aligned} \right\} \quad (47)$$

From (46) and type (47), we can see

$$\alpha_{mn} = \alpha_{nm} \quad (48)$$

$$\beta_{mn} = \beta_{nm} \tag{49}$$

**3.5 Solve the governing equations**

Dominate equations (44) and (45) are second order non-homogeneous differential equation, whose solution has the following forms:

$$N = N_0 + N' \tag{50}$$

$$M = M_0 + M' \tag{51}$$

where  $N_0$  and  $M_0$  are the generic solution of the homogeneous equations with  $N'$  and  $M'$  being the special solution of the non-homogeneous equations  $N_0$  and  $M_0$  may be exponential function:

$$N_0 = Ae^{kx} \tag{52}$$

$$M_0 = Be^{kx} \tag{53}$$

Inserting (44) and (45) into the corresponding homogeneous equation, we have

$$(\alpha_{nn}k^2 - \beta_{nn})A + (\alpha_{nm}k^2 - \beta_{nm})B = 0 \tag{54}$$

$$(\alpha_{mn}k^2 - \beta_{mn})A + (\alpha_{mm}k^2 - \beta_{mm})B = 0 \tag{55}$$

The condition for the existence of non-zero solution to these equations is that the coefficient determinant of  $A$  and  $B$  is zero.

$$\begin{vmatrix} \alpha_{nn}k^2 - \beta_{nn} & \alpha_{nm}k^2 - \beta_{nm} \\ \alpha_{mn}k^2 - \beta_{mn} & \alpha_{mm}k^2 - \beta_{mm} \end{vmatrix} = 0 \tag{56}$$

Expanding the above determinant and letting

$$a = \alpha_{nn}\alpha_{mm} - \alpha_{nm}^2 \tag{57}$$

$$b = -\alpha_{nn}\beta_{mm} - \alpha_{mm}\beta_{nn} + 2\alpha_{nm}\beta_{mn} \tag{58}$$

$$c = \beta_{nn}\beta_{mm} - \beta_{nm}^2 \tag{59}$$

We can get the following algebraic equation on  $k^2$ :

$$ak^4 + bk^2 + c = 0 \tag{60}$$

The two square roots of  $k^2$  are

$$k^2 = \frac{1}{2a} \left\{ -b \pm \sqrt{b^2 - 4ac} \right\} \tag{61}$$

For the studied spacecraft protection system tiles, the two square roots of  $k^2$  should be both real number greater than 0.

$$\kappa_1 = \mu \quad , \quad \kappa_2 = -\mu \quad (62)$$

$$\kappa_1 = \nu \quad , \quad \kappa_2 = -\nu \quad (63)$$

Where

$$\mu^2 = \frac{1}{2a} \left\{ -b + \sqrt{b^2 - 4ac} \right\} > 0 \quad (64)$$

$$\nu^2 = \frac{1}{2a} \left\{ -b - \sqrt{b^2 - 4ac} \right\} > 0 \quad (65)$$

Thus,  $N_0$  and  $M_0$  can be written in the form

$$N_0 = A_1 e^{\mu x} + A_2 e^{-\mu x} + A_3 e^{\nu x} + A_4 e^{-\nu x} \quad (66)$$

$$M_0 = B_1 e^{\mu x} + B_2 e^{-\mu x} + B_3 e^{\nu x} + B_4 e^{-\nu x} \quad (67)$$

The specific solutions for (44) and (45) of the particular solution  $N'$  and  $M'$  can be modified as

$$N' = CP \quad (68)$$

$$M' = DP \quad (69)$$

Inserting (68) and (69) into (44) and (45), one can get two algebraic equations on  $C$  and  $D$ :

$$\beta_{nn}C + \beta_{nm}D = -\beta_{np} - \frac{\beta_{nt}}{P} \quad (70)$$

$$\beta_{mn}C + \beta_{mm}D = -\beta_{mp} - \frac{\beta_{mt}}{P} \quad (71)$$

Taking into account both (70) and (71) leads to

$$C = \frac{\beta_{mn} \left( \beta_{mp} + \frac{\beta_{mt}}{P} \right) - \beta_{mm} \left( \beta_{np} + \frac{\beta_{nt}}{P} \right)}{\beta_{nn}\beta_{mm} - \beta_{mn}^2} \quad (72)$$

$$D = \frac{\beta_{nn} \left( \beta_{mp} + \frac{\beta_{mt}}{P} \right) - \beta_{mn} \left( \beta_{np} + \frac{\beta_{nt}}{P} \right)}{\beta_{mn}^2 - \beta_{nn}\beta_{mm}} \quad (73)$$

The eight undetermined coefficients depend on the following eight boundary conditions.

$$x = 0 \quad , \quad N = 0 \quad (74)$$

$$x = 0 \quad , \quad q = 0 \quad (75)$$

$$x = l, N = 0 \tag{76}$$

$$x = l, q = 0 \tag{77}$$

$$x = 0, M = 0 \tag{78}$$

$$x = 0, Q_1 = h_1q - \frac{dM}{dx} = -\frac{dM}{dx} = 0 \tag{79}$$

$$x = l, M = 0 \tag{80}$$

$$x = l, Q_1 = h_1q - \frac{dM}{dx} = -\frac{dM}{dx} = 0 \tag{81}$$

Inserting (66) and (68) into (50) and then inserting the obtained results into (74)~(77) will results in

$$A_1 + A_2 + A_3 + A_4 = -CP \tag{82}$$

$$\mu A_1 - \mu A_2 + \nu A_3 - \nu A_4 = 0 \tag{83}$$

$$e^{\mu l} A_1 + e^{-\mu l} A_2 + e^{\nu l} A_3 + e^{-\nu l} A_4 = -CP \tag{84}$$

$$\mu e^{\mu l} A_1 - \mu e^{-\mu l} A_2 + \nu e^{\nu l} A_3 - \nu e^{-\nu l} A_4 = 0 \tag{85}$$

Inserting (67) and (69) into (51) and then inserting the obtained results into (78)~(81), we have

$$B_1 + B_2 + B_3 + B_4 = -DP \tag{86}$$

$$\mu B_1 - \mu B_2 + \nu B_3 - \nu B_4 = 0 \tag{87}$$

$$e^{\mu l} B_1 + e^{-\mu l} B_2 + e^{\nu l} B_3 + e^{-\nu l} B_4 = -DP \tag{88}$$

$$\mu e^{\mu l} B_1 - \mu e^{-\mu l} B_2 + \nu e^{\nu l} B_3 - \nu e^{-\nu l} B_4 = 0 \tag{89}$$

Clearly, the generalized force  $N$  and  $M$  of TPS tiles, and the stress  $q$  and  $p$  of the layer can be calculated with the eight undetermined coefficients, which can be obtained by solving the two sets of algebraic equations.

Inserting (66), (68), (67) and (69) respectively into (50) and (51), we have

$$N = A_1 e^{\mu x} + A_2 e^{-\mu x} + A_3 e^{\nu x} + A_4 e^{-\nu x} + CP \tag{90}$$

$$M = B_1 e^{\mu x} + B_2 e^{-\mu x} + B_3 e^{\nu x} + B_4 e^{-\nu x} + DP \tag{91}$$

Further, inserting (90) and (91) into (5) and (8), we have

$$q = A_1 \mu e^{\mu x} - A_2 \mu e^{-\mu x} + A_3 \nu e^{\nu x} - A_4 \nu e^{-\nu x} \quad (92)$$

$$p = h_1 \left\{ \mu^2 (A_1 e^{\mu x} + A_2 e^{-\mu x}) + \nu^2 (A_3 e^{\nu x} + A_4 e^{-\nu x}) \right\} - \left\{ \mu^2 (B_1 e^{\mu x} + B_2 e^{-\mu x}) + \nu^2 (B_3 e^{\nu x} + B_4 e^{-\nu x}) \right\} \quad (93)$$

which are the closed solution for the stress of the layer.

#### 4. Consequence analyses

By this analysis, solving layer stress can be summarized in the following procedure:

- i. Based on (23)~(26), write (17) and (20).
- ii. Calculate the coefficients in (60) with (57), (58) and (59).
- iii. Get (76) and (77) based on (64) and (65).
- iv. According to (70) and (71), particular solutions of inhomogeneous equation are shown as the coefficient of (68) and (69).
- v. Calculate every coefficients of generic solution for the homogeneous equation to get the distribution of stress of the layer.

From the mechanical point of view, based on the above theoretical derivation, in order to have more detailed understanding of the "Peeling off" problem for TPS tiles on space craft surfacethe, the maximum potential peeling stress was analyzed in its working condition, the effects of the outside aerodynamic heating and the tiles size design on the peeling stress are investigated.

As we all know, the material of spacecraft structure is mainly aluminium and its alloy materials. The mechanical properties of aluminium alloy can be found from "mechanical Dictionary" (The editorial department of Mechanical dictionary., 1990):  $E=70\sim 79\text{GPa}$ ,  $G=26\sim 30\text{GPa}$ ,  $\sigma_s=35\sim 500\text{MPa}$ ,  $\sigma_b=100\sim 550\text{MPa}$ , thermal expansion coefficient  $\alpha = 2.3 \times 10^{-5} / ^\circ\text{C}$ . The material of rigid TPS tiles shown in Figure 2 is mainly the ceramic or ceramic-based materials. From (Davis., 2003), TPS tiles is mainly made of  $\text{SiC}$  and  $\text{SiO}_2$ , whose mechanical properties are that  $E=95\sim 402\text{GPa}$ , thermal expansion coefficient  $\alpha = 3.8 \sim 7.4 \times 10^{-6} / ^\circ\text{C}$ . In the following stress distribution, the dimensionless coordinates are established based on Figure 6, where  $x'' = x' / h_2$ ,  $q' = q h_2 / P$ ,  $p' = p h_2 / P$ .

##### 4.1 Different aerodynamic heating temperature on the peeling stress

The external TPS of re-entering body will have a high temperature during the spacecraft re-entering atmosphere with high aerodynamic heating, resulting thermal deformation of TPS tiles. Hence it is necessary that the effects of the outside aerodynamic heating on the peeling stress are investigated by theoretical analysis discussed above.

When the spacecraft returns to the atmosphere at high speed, the aerodynamic heating will lead to high temperature of the spacecraft re-entry body's external thermal protection system, thereby enabling protection watt thermal deformation. To study the effect of aerodynamic heating on the TPS tiles peeling stress by the above theory, we let the working stress of the structure  $P=20\text{MPa}$  and take  $E_1=E_2$ ,  $h_1=0.5h_2$ ,  $t_0=20^\circ\text{C}$ ,  $t_{j0}=177^\circ\text{C}$ , when the outside temperature of TPS tiles with aerodynamic heating  $t_1=177^\circ\text{C}$ ,  $300^\circ\text{C}$ ,  $500^\circ\text{C}$ ,  $700^\circ\text{C}$ ,  $1000^\circ\text{C}$ , and then get the distribution of the shear and normal stress of the adhesive layer, as shown in Figures 6, 7 and 8.

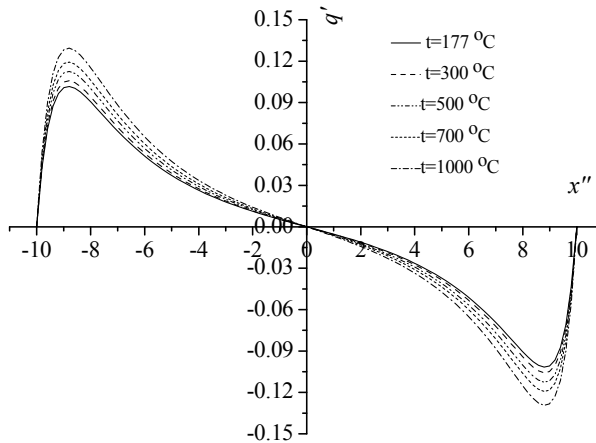


Fig. 6. Distribution of shearing stress  $q'$  along the glue layer with different  $t_1$

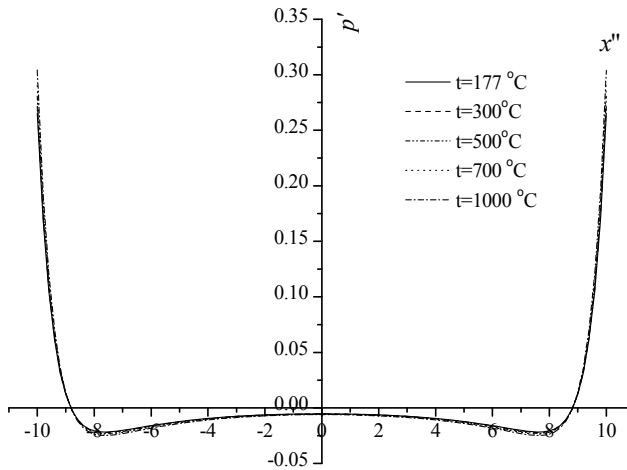


Fig. 7. Distribution of shearing stress  $p'$  along the glue layer with different  $t_1$

**4.2 The effects of the length of TPS tiles on peeling stress**

Here, the effects of the length of the TPS tiles on the glue layer stress were Investigated. Here, we examine the effect of the length of TPS tiles on stress distribution of the adhesive layer. Let the working stress of the structure  $P=20\text{MPa}$ , and  $E_1 = 2E_2$ ,  $h_1 = 0.5h_2$ ,  $t_0 = 20^\circ\text{C}$ ,  $t_{j0} = 177^\circ\text{C}$ ,  $t_1 = 500^\circ\text{C}$ . When  $L/h_2 = 4, 6, 10, 15,$  and  $20$ , by the above theory, we get the distribution of shear and normal stress, as shown in Figures 9 and 10.

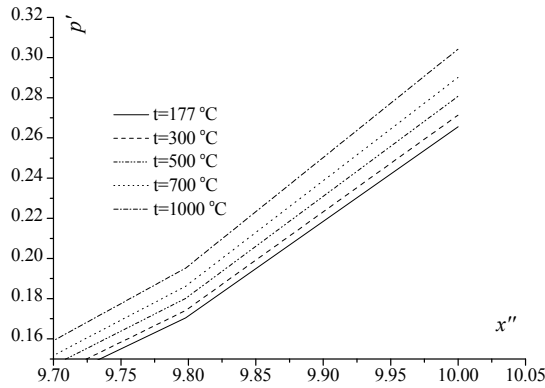


Fig. 8. Distribution of shearing stress  $p'$  along the glue layer with different  $t_1$  (part curve)

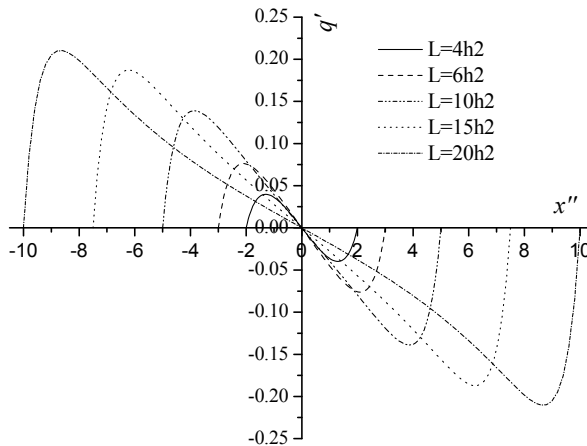


Fig. 9. Distribution of shearing stress  $q'$  along the glue layer with different length for TPS tiles

**4.3 The effects of the thickness of TPS tiles on peeling stress**

The thickness of the tiles in TPS design was also a very important consideration. The thickness of TPS tile thermal protection system in the design is also a very important consideration. We should analyze the effect of the TPS tiles thickness on the shear and normal stress of the layer. Let the working stress of the structure  $P=20\text{MPa}$ , and  $E_1=2E_2$ ,  $L=10 h_2$ ,  $t_0=20^\circ\text{C}$ ,  $t_j=177^\circ\text{C}$ ,  $t_1=500^\circ\text{C}$ . When  $h_1/h_2= 1/2, 1/3, 1/5, 1/8$ , by the above theory, we also get the distribution of shear and normal stress, as shown Figures 11 and 12 respectively.



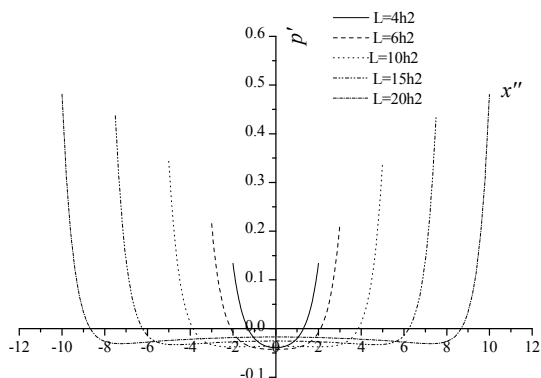


Fig. 10. Distribution of shearing stress  $p'$  along the glue layer with different length for TPS tiles

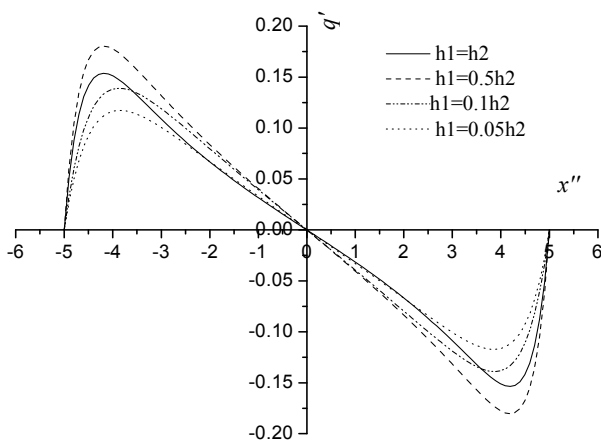


Fig. 11. Distribution of shearing stress  $q'$  along the glue layer with different thickness for TPS tiles

#### 4.4 The effects of the material of TPS tiles on peeling stress

The selected material is different in different spacecraft TPS.

For different thermal systems of spacecraft, the selection of protection tile material is also different. Here, from a mechanical point of view, we study the effects of different material on the thermal protection tiles peeling off, i.e. the adhesive layer stress, mainly considering the effect of elastic modulus. Let the working stress of the structure  $P=20\text{MPa}$ , and  $h_1/h_2=0.5$ ,  $L=10 h_2$ ,  $t_0=20^\circ\text{C}$ ,  $t_{j0}=177^\circ\text{C}$ ,  $t_1=500^\circ\text{C}$ . When  $E_1/E_2=0.5, 1, 2,$  and  $3$ , by the above theory, we also get the distribution of shear and normal stress, as shown Figures 13, 14 and 15 respectively.

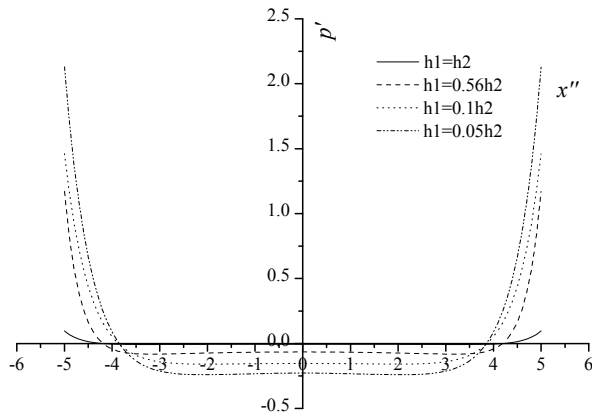


Fig. 12. Distribution of shearing stress  $p'$  along the glue layer with different thickness for TPS tiles

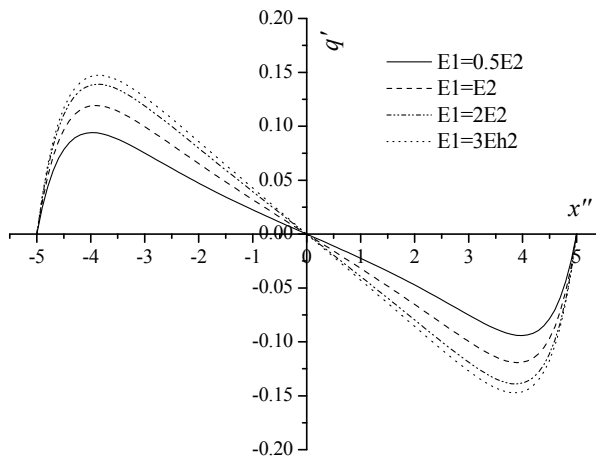


Fig. 13. Distribution of shearing stress  $q'$  along the glue layer with different materials for TPS tiles

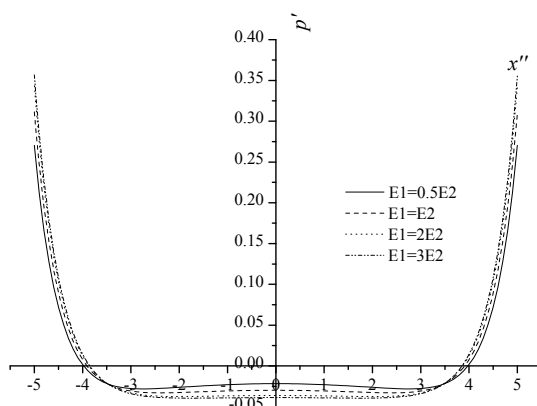


Fig. 14. Distribution of shearing stress  $p'$  along the glue layer with different materials for TPS tiles

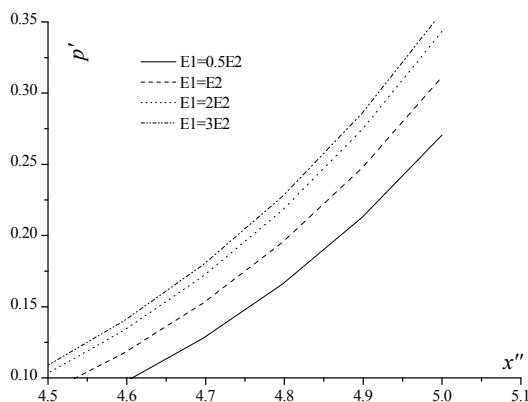


Fig. 16. Distribution of shearing stress  $p'$  along the glue layer with different materials for TPS tiles (part curve)

### 5. Conclusions

By analyzing the glue layer stress between TPS tiles and structures, and the influence of the size and material of TPS tiles, we concludes:

1. In the connection between TPS tiles and internal structure, the normal stress on the glue layer end reaches the max value with naught shear stress. Hence, it can be indicated that potential factors of the peeling off of the tiles are mainly contributed by peeling normal stress and influenced little by shear stress.

2. Glue layer stress concentrates near the edge of the tiles and almost naught in other areas. The fact that the ratios of glue layer shear stress and normal stress to working stress decreases with increasing working stress in the inner structure indicates that the increasing rate of glue layer stress is less than that of working stress.
3. Glue layer shear stress and normal stress both increases with temperature increasing, however, the increasing magnitude is not very large compared to influence of working stress's increasing on peeling stress, which also illustrates that the more aerodynamic heating is, the larger peeling stress of tiles is, quickening the desquamation of tiles.
4. Glue layer shear stress and normal stress concentrates much more near the end of tiles and their extremum get larger as the length of TPS tilse increases; furthermore, the shear stress varies much more. This fact indicates that larger size of TPS tiles leads to peeling stress of glue larger and the influence of the length of the TPS tiles on the extremum of glue layer stress is obvious.
5. However, glue layer stress does not decrease (or increase) as the thickness of TPS tiles decreases (or increases). The thickness of TPS tiles does not influence the extremum of glue layer shear stress obviously, but much glue layer normal stress.
6. The influence of material Elastic modulus on peeling stress of glue layer is not strong, however, as a whole, the larger material Elastic modulus (i.e. Stiffness) is, the larger peeling stress of glue layer is.

## 6. References

- XING Yu-zhe., 2003. The final investigation report of columbia disaster[J].*Spece Exploration*, pp. 12:18-19.
- Kuhn P., 1956. *Stress in Aircraft and Structures*[M].McCraw-HIHLL BOOK COMPANY,
- ZANG Qing-lai, ZHANG Xing, WU Guo-xun. (2006). New model and new method of stress analysis about glued joints[J].*Chinese Journal of Aeronautics*, pp.6:1051-1057.
- Timoshenko S., 1958. *Strength of Materials*[M].Van Nostrand Reinhold Company.
- HU Hai-chang., 1980. *Variational Principle and Application in Theory of Elasticity*[M]. Beijing:Science Press.
- ZHANG Xing (editor in chief),, 1995. *Advanced Theory of Elas-ticity* [M]. Beijing:Beijing University of Aeronautics and Astronautics Press.
- QIAN Wei-chang., 1980. *Variational Method and finite Element*[M].Beijing:Sci-enee Press.
- The editorial department of Mechanical dic-tionary., 1990. *Mechanical Dietinary* [M]. Beijing:Encyclopedia of China Publishing House, pp.197-597.
- Davis J,Green, translted by Gong Jiang-hong., 2003. *The Mechanical Properties Introduction of Ceramic Materials*[M].Beijing:Tsinghua University Press, pp.21-35.]



## **Advances in Spacecraft Technologies**

Edited by Dr Jason Hall

ISBN 978-953-307-551-8

Hard cover, 596 pages

**Publisher** InTech

**Published online** 14, February, 2011

**Published in print edition** February, 2011

The development and launch of the first artificial satellite Sputnik more than five decades ago propelled both the scientific and engineering communities to new heights as they worked together to develop novel solutions to the challenges of spacecraft system design. This symbiotic relationship has brought significant technological advances that have enabled the design of systems that can withstand the rigors of space while providing valuable space-based services. With its 26 chapters divided into three sections, this book brings together critical contributions from renowned international researchers to provide an outstanding survey of recent advances in spacecraft technologies. The first section includes nine chapters that focus on innovative hardware technologies while the next section is comprised of seven chapters that center on cutting-edge state estimation techniques. The final section contains eleven chapters that present a series of novel control methods for spacecraft orbit and attitude control.

### **How to reference**

In order to correctly reference this scholarly work, feel free to copy and paste the following:

Zhang Taihua, Meng Xianhong and Zhang Xing (2011). The Mechanics Analysis of Desquamation for Thermal Protection System (TPS) Tiles of Spacecraft, *Advances in Spacecraft Technologies*, Dr Jason Hall (Ed.), ISBN: 978-953-307-551-8, InTech, Available from: <http://www.intechopen.com/books/advances-in-spacecraft-technologies/the-mechanics-analysis-of-desquamation-for-thermal-protection-system-tps-tiles-of-spacecraft>

# **INTECH**

open science | open minds

### **InTech Europe**

University Campus STeP Ri  
Slavka Krautzeka 83/A  
51000 Rijeka, Croatia  
Phone: +385 (51) 770 447  
Fax: +385 (51) 686 166  
[www.intechopen.com](http://www.intechopen.com)

### **InTech China**

Unit 405, Office Block, Hotel Equatorial Shanghai  
No.65, Yan An Road (West), Shanghai, 200040, China  
中国上海市延安西路65号上海国际贵都大饭店办公楼405单元  
Phone: +86-21-62489820  
Fax: +86-21-62489821

© 2011 The Author(s). Licensee IntechOpen. This chapter is distributed under the terms of the [Creative Commons Attribution-NonCommercial-ShareAlike-3.0 License](#), which permits use, distribution and reproduction for non-commercial purposes, provided the original is properly cited and derivative works building on this content are distributed under the same license.